USGS
science for a changing world

Isotopic Data for Late Cretaceous Intrusions and Associated Altered and Mineralized Rocks in the Big Belt Mountains, Montana

Data Series 1040

U.S. Department of the Interior
U.S. Geological Survey

Cover. Prominent granitoid outcrops at The Needles, Big Belt Mountains, Montana. (Photo by Edward A. du Bray, U.S. Geological Survey, 1993)

Isotopic Data for Late Cretaceous Intrusions and Associated Altered and Mineralized Rocks in the Big Belt Mountains, Montana

By Edward A. du Bray, Daniel M. Unruh, and Albert H. Hofstra

Data Series 1040

U.S. Department of the Interior
U.S. Geological Survey

U.S. Department of the Interior
RYAN K. ZINKE, Secretary

U.S. Geological Survey
William H. Werkheiser, Acting Director

U.S. Geological Survey, Reston, Virginia: 2017

Suggested citation:
du Bray, E.A., Unruh, D.M., and Hofstra, A.H., 2017, Isotopic data for Late Cretaceous intrusions and associated altered and mineralized rocks in the Big Belt Mountains, Montana: U.S. Geological Survey Data Series 1040, 12 p., https://doi.org/10.3133/ds1040.

ISSN 2327-638X (online)

Contents

Figures

Tables

Isotopic Data for Late Cretaceous Intrusions and Associated Altered and Mineralized Rocks in the Big Belt Mountains, Montana

By Edward A. du Bray, Daniel M. Unruh, and Albert H. Hofstra

Abstract

The quartz monzodiorite of Mount Edith and the concentrically zoned intrusive suite of Boulder Baldy constitute the principal Late Cretaceous igneous intrusions hosted by Mesoproterozoic sedimentary rocks of the Newland Formation in the Big Belt Mountains, Montana. These calc-alkaline plutonic masses are manifestations of subduction-related magmatism that prevailed along the western edge of North America during the Cretaceous. Radiogenic isotope data for neodymium, strontium, and lead indicate that the petrogenesis of the associated magmas involved a combination of (1) sources that were compositionally heterogeneous at the scale of the geographically restricted intrusive rocks in the Big Belt Mountains and (2) variable contamination by crustal assimilants also having diverse isotopic compositions. Altered and mineralized rocks temporally, spatially, and genetically related to these intrusions manifest at least two isotopically distinct mineralizing events, both of which involve major inputs from spatially associated Late Cretaceous igneous rocks. Alteration and mineralization of rock associated with the intrusive suite of Boulder Baldy requires a component characterized by significantly more radiogenic strontium than that characteristic of the associated igneous rocks. However, the source of such a component was not identified in the Big Belt Mountains. Similarly, altered and mineralized rocks associated with the quartz monzodiorite of Mount Edith include a component characterized by significantly more radiogenic strontium and lead, particularly as defined by $^{207}Pb/^{204}Pb$ values. The source of this component appears to be fluids that equilibrated with proximal Newland Formation rocks. Oxygen isotope data for rocks of the intrusive suite of Boulder Baldy are similar to those of subduction-related magmatism that include mantle-derived components; oxygen isotope data for altered and mineralized equivalents are slightly lighter.

Introduction

The Big Belt Mountains in western Montana, about 50 kilometers (31 miles) southeast of Helena, host two areally significant Late Cretaceous plutons: (1) the intrusive suite of Boulder Baldy in the northern part of the Big Belt Mountains and (2) the quartz monzodiorite of Mount Edith in the southern part of the mountain range (fig. 1). Geochemical and geologic relations suggest that these calc-alkaline intrusions are related to subduction and back-arc processes that prevailed along the late Mesozoic margin of western North America (du Bray and Snee, 2002). The distribution, geochronology, and petrogenesis of these plutonic masses is thoroughly documented by du Bray (1995) and du Bray and Snee (2002). The intrusive suite of Boulder Baldy constitutes a discontinuously compositionally zoned pluton, whereas the Mount Edith pluton is composed of relatively homogeneous quartz monzodiorite. The intrusive suite of Boulder Baldy consists of a core zone composed of biotite granodiorite, an intermediate zone composed of hornblende quartz monzodiorite, and an outer zone composed of variably altered granitoid rock whose primary composition is indeterminate. Geochemical compositions and petrographic characteristics of the intermediate zone of the intrusive suite of Boulder Baldy and the quartz monzodiorite of Mount Edith are similar. New $^{40}Ar/^{39}Ar$ geochronologic data suggest that magmas associated with both plutons solidified about 68 Ma (du Bray and Snee, 2002), which is consistent with a 66.2±0.9 Ma U-Pb age for zircon from a sample of the intermediate zone of the intrusive suite of Boulder Baldy (Lund and others, 2002).

Unusual textures, odd mineralogy, and erratic compositional variation in the outer part of the intrusive suite of Boulder Baldy reflect extensive hydrothermal alteration and recrystallization of granitoid rock by metal-bearing fluid. The distribution and character of small precious metal deposits and associated placer deposits are described by du Bray and Snee (1995). These altered and mineralized rocks are important because they bear similarities to certain intrusions with associated gold deposits located elsewhere in the world (Lang and others, 2000). Isotopic data presented in this report were obtained in order to constrain the source and character of fluids responsible for hydrothermal alteration and mineralization in the vicinity of these two plutons (table 1).

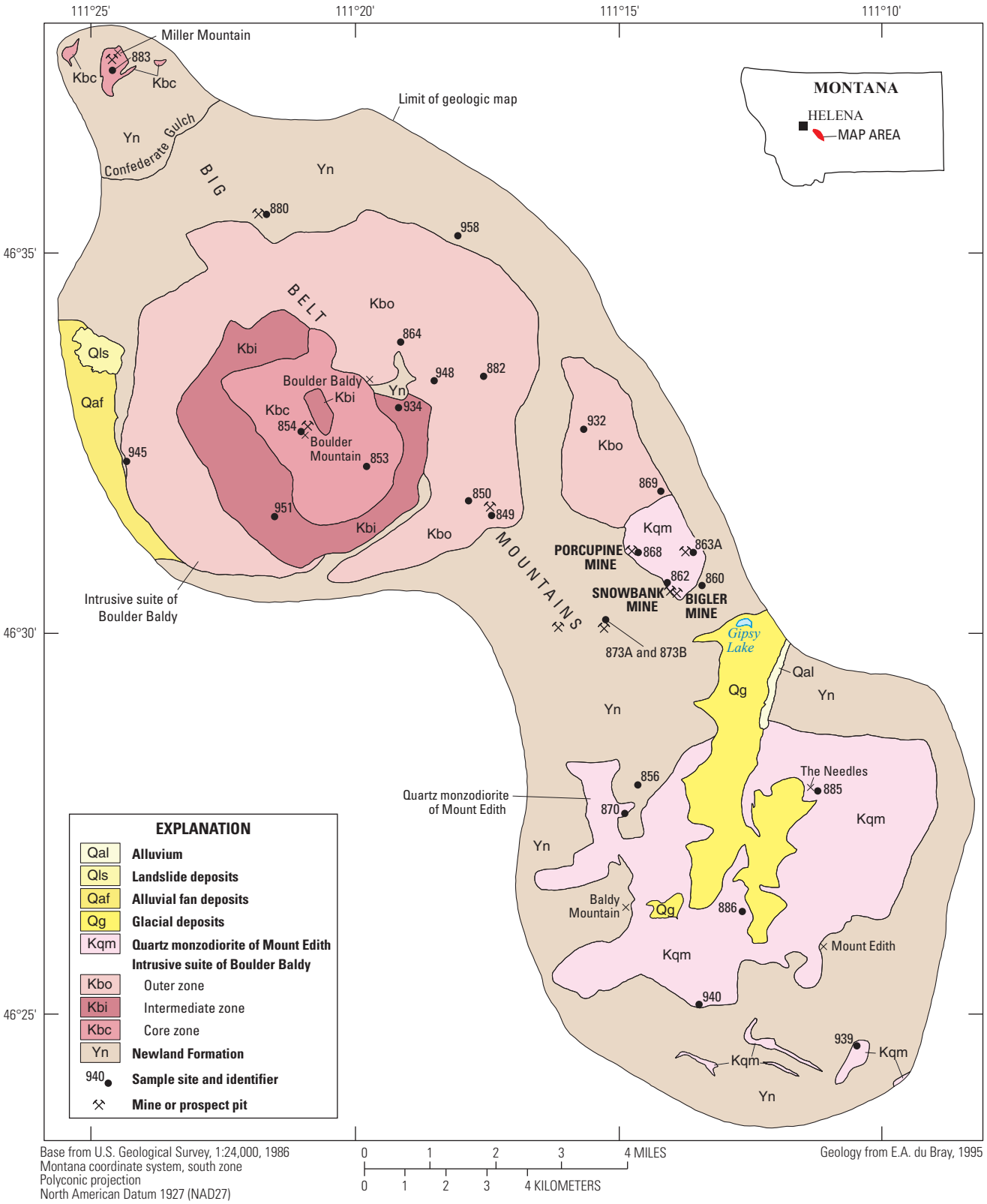

Figure 1. Distribution of Late Cretaceous intrusive rocks in the central Big Belt Mountains, Montana (From du Bray, 1995). Sample numbers (at localities indicated by plus signs) must be prefaced by 202 to obtain complete designations. Only samples for which isotopic data have been obtained are shown.

Table 1. Locations and descriptions for selected samples from the Big Belt Mountains, Montana.

Sample	Longitude	Latitude	Rock type
202854	–111.35056	46.54389	Core zone, intrusive suite of Boulder Baldy: biotite granodiorite
202853	–111.32972	46.53639	Core zone, intrusive suite of Boulder Baldy: biotite granodiorite
202934	–111.31944	46.54917	Intermediate zone, intrusive suite of Boulder Baldy: hornblende quartz monzodiorite
202951	–111.35889	46.52528	Intermediate zone, intrusive suite of Boulder Baldy: hornblende quartz monzodiorite
202945	–111.40583	46.5375	Outer zone, intrusive suite of Boulder Baldy: monzodiorite, magmatic texture
202864	–111.31889	46.56361	Outer zone, intrusive suite of Boulder Baldy: quartz monzonite, magmatic texture
202882	–111.29250	46.55611	Outer zone, intrusive suite of Boulder Baldy: aegirine quartz monzonite, partly recrystallized
202932	–111.26083	46.54444	Outer zone, intrusive suite of Boulder Baldy: quartz syenite, partly recrystallized/metasomatized
202948	–111.30833	46.555	Outer zone, intrusive suite of Boulder Baldy: pegmatitic, in part
202850	–111.29750	46.52889	Crowded feldspar rock, intrusive suite of Boulder Baldy
202869	–111.23639	46.53083	Crowded feldspar rock, intrusive suite of Boulder Baldy
202883	–111.41028	46.62278	Weakly mineralized granodiorite/quartz monzodiorite of Miller Mountain
202870	–111.24806	46.46056	Hornblende quartz monzodiorite of Mount Edith
202885	–111.18694	46.46528	Hornblende quartz monzodiorite of Mount Edith
202886	–111.21083	46.43889	Hornblende quartz monzodiorite of Mount Edith
202939	–111.17556	46.40944	Feldspar porphyry south of Mount Edith
202958	–111.30083	46.59028	Proterozoic lamprophyre dike
202863A	–111.22889	46.5175	Weakly mineralized rock from Porcupine prospect; iron stained
202849	–111.29056	46.5275	Fluorite at Normandy prospect
202868	–111.24583	46.51778	Mineralized hornblende quartz monzodiorite, Little Camas mine
202873A	–111.25472	46.50083	Quartz vein in quartzite of Newland Formation, massive
202873B	–111.25472	46.50083	Iron oxide on fractures in quartzite of Newland Formation
202880	–111.36417	46.59167	Iron oxide on fractures
202860	–111.22611	46.50861	Iron-stained Newland Formation rock at Bigler prospect
202862	–111.23361	46.50917	Altered Newland Formation rock at Snowbank prospect
202856	–111.24333	46.46361	Quartzite of Newland Formation, with pyrite

Analytical Methods

Oxygen-stable isotope analyses were performed at the U.S. Geological Survey Stable Isotope Laboratory in Denver, Colorado. Several milligrams of powdered rock were digested using bromine pentafluoride and the oxygen generated was converted to carbon dioxide by reaction with carbon as described by Clayton and Mayeda (1963). The carbon dioxide samples were analyzed for their isotopic compositions using a Finnigan MAT 252 mass spectrometer; analytical precision generally was better than ±0.2 percent. The results are reported in delta notation in units of per mil relative to Vienna Standard Mean Ocean Water.

Whole-rock splits of each sample were spiked with ^{205}Pb-^{233}U-^{236}U-^{230}Th-, ^{87}Rb-^{84}Sr-, and ^{149}Sm-^{150}Nd-enriched tracers and were digested in PFA-Teflon screw-cap bombs with hydrogen fluoride and nitric acid for a minimum of 48 hours at approximately 120 °C. Lead (Pb) was isolated first using anion exchange in 0.5N hydrobromic acid medium. Anion exchange, in a 7N nitric acid medium, was used to separate uranium (U) and thorium (Th). Rubidium (Rb), strontium (Sr), and a rare earth fraction were isolated using cation exchange in a 2.5N hydrochloric acid medium. Samarium (Sm) and neodymium (Nd) were separated from the rare earth fraction using cation exchange in 0.2M n-methyllactic acid. Blanks for the procedure were on the order of Pb–50 picograms (pg), U and Th–15 pg, Rb–40 pg, Sr–300 pg, Sm–50 pg, and Nd–300 pg.

Mass spectrometry for U, Th, and Pb was performed using either a VG Sector 54 seven-collector thermal ionization mass spectrometer or a VG54R single-collector mass spectrometer. Mass fractionation for Pb during mass spectrometry was monitored by replicate analyses using National Institute of Standards and Technology standard SRM-981—Common Lead Isotopic Standard (Cantanzaro and others, 1968; Todt and others, 1993). A VG 54R single-collector mass spectrometer was used to analyze for Rb, Sr, Sm, and Nd. The

Rb analysis was conducted using a triple rhenium filament technique, Sr was analyzed using a single oxidized tantalum filament, and Sm and Nd were determined using a triple filament technique with a rhenium ionizing filament and tantalum sample filaments. Data reduction was accomplished using the equations of Ludwig (1994). Uncertainties in the data tables are at the 95 percent confidence interval.

Stable Isotope Data

Investigations by Taylor (1968) and Bindeman (2008) determined that most common, subduction-related igneous rocks whose petrogenesis includes significant mantle-derived inputs have delta-oxygen-18 ($\delta^{18}O$) values restricted to the 5–10 per mil range. Selected samples from the intrusive suite of Boulder Baldy for which oxygen isotope data are available have $\delta^{18}O$ values within this range (table 2). Two samples from the outer zone of the intrusive suite of Boulder Baldy that were identified as having been partly recrystallized and altered by hydrothermal fluids have subtly, but systematically, lower $\delta^{18}O$ values than unaltered samples. Oxygen isotope data for these two samples are consistent with hydrothermal alteration and exchange with a fluid consisting of magmatic water with a minor component of meteoric water.

Table 2. Oxygen isotope compositions of selected samples from the Big Belt Mountains, Montana.

[$\delta^{18}O$, delta-oxygen-18; ‰, per mil]

Sample	Rock type	$\delta^{18}O$ in ‰
202854	Core zone, Boulder Baldy pluton	8.1
202934	Intermediate zone, Boulder Baldy pluton	7.8
202864	Outer zone, Boulder Baldy pluton, magmatic texture	8.2
202945	Outer zone, Boulder Baldy pluton, magmatic texture	8.5
202882	Outer zone, Boulder Baldy pluton, partly recrystallized	7.3
202932	Outer zone, Boulder Baldy pluton, partly recrystallized	7.7

Radiogenic Isotope Data

Local Systematics

Late Cretaceous igneous rocks in the Big Belt Mountains have surprisingly diverse radiogenic isotopic characteristics (tables 3 and 4). Given the proximity of plutons represented by the intrusive suite of Boulder Baldy and the quartz monzodiorite of Mount Edith, and therefore the likelihood that their associated magma reservoirs had similar sources and evolved by similar processes, their mutually distinctive isotopic compositions are noteworthy. Although the initial strontium isotope ratios (Sr_i) for these two sets of igneous rocks are similar, corresponding epsilon neodymium (ε_{Nd}) values are quite distinct (fig. 2). The Sr_i values for all of these rocks are restricted to a narrow range from about 0.7045 to 0.7067, but ε_{Nd} values for the quartz monzodiorite of Mount Edith range from –13.27 to –17.84 and ε_{Nd} values for most of the intrusive suite of Boulder Baldy range from about –3.91 to –8.84. The ε_{Nd} values for the intrusive suite of Boulder Baldy rocks vary systematically from –16.56 to –18.18 in the core zone, to –7.06 to –7.76 in the intermediate zone, to –3.91 to –8.84 in the outer zone. Initial Pb isotope data (table 4) confirm that the quartz monzodiorite of Mount Edith and the intrusive suite of Boulder Baldy rocks are isotopically distinct (fig. 3) and that the isotopic ratios of rocks from the three zones of the intrusive suite of Boulder Baldy vary extensively.

The ε_{Nd} and Sr_i values for the core zone of the intrusive suite of Boulder Baldy and quartz monzodiorite of Mount Edith are essentially indistinguishable. In contrast, Pb isotope data for the intermediate zone and the quartz monzodiorite of Mount Edith are similar. Consequently, the Nd and Sr isotopic systems and the Pb isotopic system were decoupled as they pertain to petrogenetic relations between magmas represented by the quartz monzodiorite of Mount Edith and the core and intermediate zones of the intrusive suite of Boulder Baldy.

Initial Pb, Sr, and Nd isotopic compositions also constrain relations between the principal plutonic rocks and volumetrically minor intrusive bodies in the Big Belt Mountains. Isotopic values (figs. 2–5) of the quartz monzodiorite of Mount Edith, feldspar porphyry masses on the south flank of Mount Edith, and the small porphyritic stock at Miller Mountain (fig. 1) are indistinguishable; consequently, these intrusions have similar sources and petrogenetic histories. In contrast, texturally unusual rocks (crowded feldspar rocks described by du Bray and Snee, 2002) that consist almost entirely of aligned, densely packed euhedral perthite phenocrysts have initial Pb, Sr, and Nd isotopic values indistinguishable from those for the outer zone of the intrusive suite of Boulder Baldy. Consequently, the source of Pb, Sr, and Nd in hydrothermal fluids responsible for alteration of the outer zone rocks likely also contributed to the formation of the crowded feldspar rocks. Predictably, initial Pb, Sr, and Nd isotopic values of a thick, northwest-trending late Proterozoic mafic dike in the northeast part of the Big Belt Mountains are unique relative to all other samples; thus, the mafic dike does

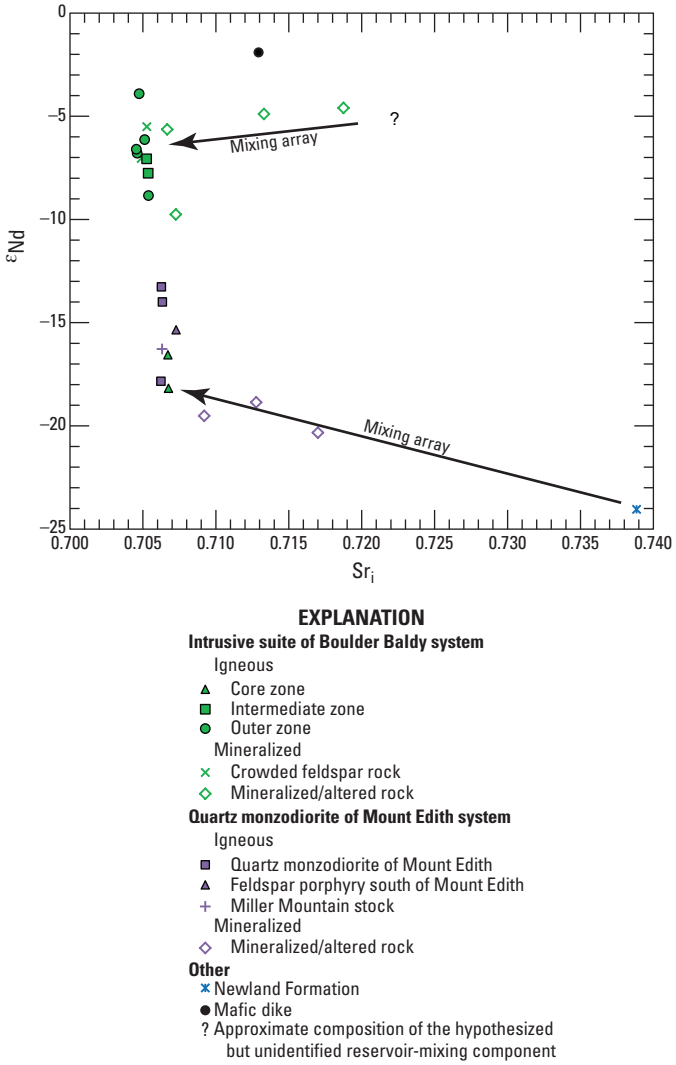

Figure 2. Variation diagram showing ε_{Nd} and Sr_i values for intrusive rocks in the central Big Belt Mountains, Montana. (ε_{Nd}, epsilon neodymium; Sr_i, initial strontium isotope ratio)

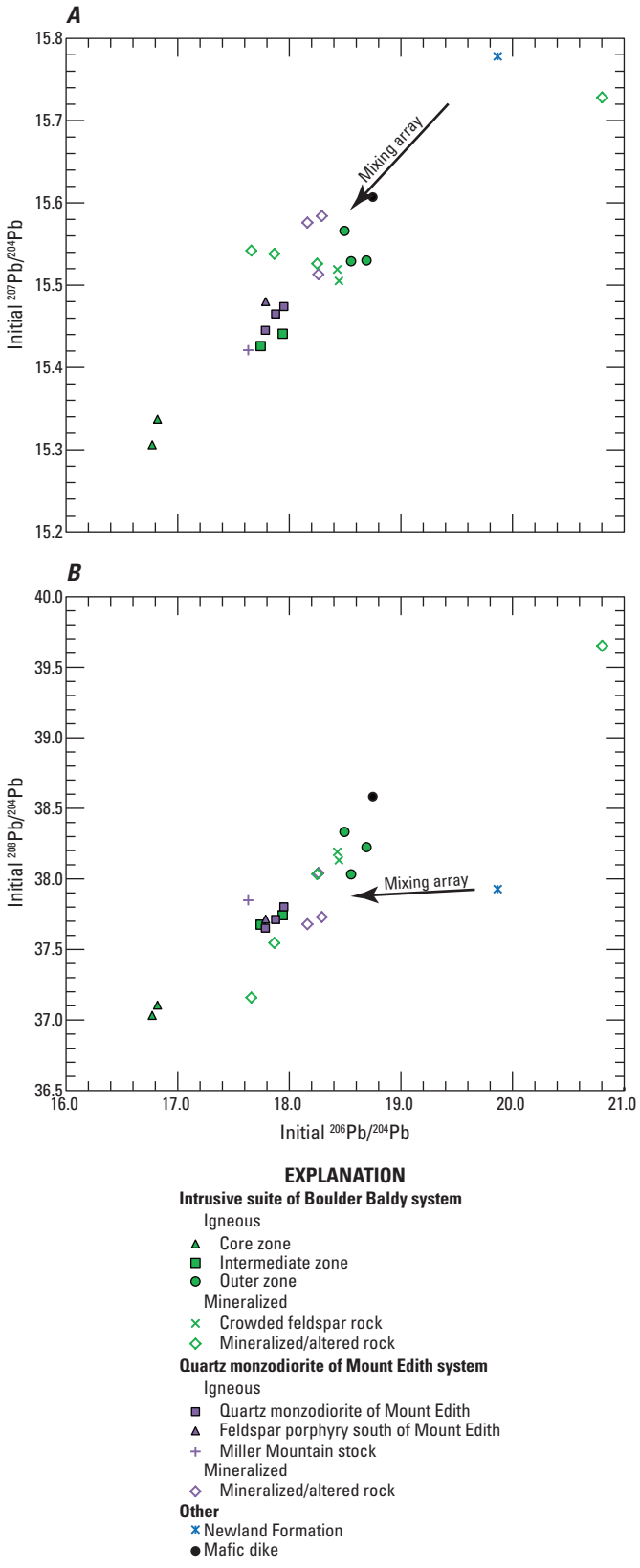

Figure 3. Variation diagrams showing initial lead isotopic compositions of intrusive rocks in the central Big Belt Mountains, Montana. *A*, Initial $^{207}Pb/^{204}Pb$ versus initial $^{206}Pb/^{204}Pb$. *B*, Initial $^{208}Pb/^{204}Pb$ versus initial $^{206}Pb/^{204}Pb$. (Pb, lead)

not appear to have contributed to the petrogenesis of the Late Cretaceous magmas in the area or to the fluids responsible for hydrothermal alteration and mineralization.

Radiogenic isotope data, especially ε_{Nd} and Sr_i values, suggest that two isotopically distinct fluid sources are involved in mineralizing events in the Big Belt Mountains. Three vein and mineralized rock samples from the southern part of the Big Belt Mountains, which are spatially associated with the quartz monzodiorite of Mount Edith pluton, have elevated ε_{Nd} and Sr_i values that define a mixing array between values typical of the quartz monzodiorite and those of unmineralized Newland Formation rocks (figs. 2 and 3). Because the isotopic values of these samples are more similar to those of the quartz monzodiorite than they are to Newland Formation rocks, contributions from the Newland Formation are probably less significant. The single Newland Formation sample has dramatically more radiogenic Sr, and somewhat more

Table 3. Rubidium, strontium, samarium, and neodymium concentrations; and strontium and neodymium isotopic compositions of selected samples from the Big Belt Mountains, Montana.

[ε_{Nd}, epsilon neodymium; Ga, giga-annum; Ma, mega-annum; Nd, neodymium; ppm, parts per million; Rb, rubidium; Sm, samarium; Sr, strontium; T_{DM}, depleted mantle model age]

Sample	Formation[1]	Rb ppm	Sr ppm	Sm ppm	Nd ppm	$^{87}Rb/^{86}Sr$	$^{87}Sr/^{86}Sr$	$^{147}Sm/^{144}Nd$	$^{143}Nd/^{144}Nd$	ε_{Nd}	Initial $^{87}Sr/^{86}Sr$	Initial $^{143}Nd/^{144}Nd$[3]	Initial ε_{Nd}[2,3]	T_{DM} (Ga)[4]
202870	Hornblende quartz monzodiorite of Mount Edith	81.1	978.7	2.66	15.3	0.2398 ± 0.0027	0.706470 ± 0.000021	0.10503 ± 0.00011	0.511912 ± 0.000014	–14.12	0.706245 ± 0.000021	0.511637 ± 0.000014	–17.84	1.57
202885	Hornblende quartz monzodiorite of Mount Edith	113.6	778.5	2.05	11.73	0.4223 ± 0.0331	0.706736 ± 0.000012	0.10557 ± 0.00035	0.511879 ± 0.000025	–14.77	0.706340 ± 0.000033	0.511833 ± 0.000025	–14.00	1.63
202886	Hornblende quartz monzodiorite of Mount Edith	113.7	873.8	1.92	10.9	0.3765 ± 0.0327	0.706618 ± 0.000029	0.10642 ± 0.00049	0.511917 ± 0.000015	–14.03	0.706265 ± 0.000042	0.511871 ± 0.000015	–13.27	1.59
202854	Core/inner zone Boulder Baldy pluton: biotite granodiorite	54.5	565.6	2.33	14.87	0.2785 ± 0.0032	0.706979 ± 0.000012	0.09465 ± 0.00283	0.511743 ± 0.000015	–17.42	0.706718 ± 0.000012	0.511702 ± 0.000015	–16.56	1.65
202853	Core/inner zone Boulder Baldy pluton: biotite granodiorite	57.6	604.1	1.43	6.43	0.2758 ± 0.0108	0.707011 ± 0.000020	0.13405 ± 0.00034	0.511677 ± 0.000023	–18.71	0.706752 ± 0.000022	0.511619 ± 0.000023	–18.18	2.61
202934	Intermediate zone Boulder Baldy pluton: hornblende quartz monzodiorite	96.9	1404	4.59	25.02	0.1996 ± 0.0015	0.705543 ± 0.000021	0.11069 ± 0.00035	0.512201 ± 0.000030	–8.49	0.705356 ± 0.000021	0.512153 ± 0.000030	–7.76	1.24
202951	Intermediate zone Boulder Baldy pluton: hornblende quartz monzodiorite	103.6	1005	2.24	12.98	0.2980 ± 0.0198	0.705530 ± 0.000029	0.10395 ± 0.00042	0.512234 ± 0.000017	–7.84	0.705251 ± 0.000034	0.512189 ± 0.000017	–7.06	1.12
202945	Outer zone Boulder Baldy pluton: monzodiorite, magmatic texture	92.7	1250	4.05	26.46	0.2145 ± 0.0015	0.705578 ± 0.000020	0.09233 ± 0.00016	0.512138 ± 0.000012	–9.71	0.705377 ± 0.000020	0.512098 ± 0.000012	–8.84	1.13
202864	Outer zone Boulder Baldy pluton: quartz monzonite, magmatic texture	93.9	31.0	0.37	2.85	8.7735 ± 0.0622	0.712830 ± 0.000034	0.07833 ± 0.00075	0.512237 ± 0.000024	–7.78	0.704604 ± 0.000068	0.512203 ± 0.000024	–6.79	0.91
202882	Outer zone Boulder Baldy pluton: aegirine quartz monzonite, partly recrystallized	84.1	46.4	0.94	12.02	5.2469 ± 0.0340	0.709462 ± 0.000021	0.04731 ± 0.00015	0.512233 ± 0.000015	–7.86	0.704542 ± 0.000038	0.512213 ± 0.000015	–6.60	0.75
202932	Outer zone Boulder Baldy pluton: quartz syenite, recrystallized and metasomatized	131.5	1842	6.26	39.66	0.2065 ± 0.0018	0.704930 ± 0.000023	0.09527 ± 0.00041	0.512392 ± 0.000015	–4.76	0.704736 ± 0.000023	0.512351 ± 0.000015	–3.91	0.84
202948	Aplite from outer zone of Boulder Baldy pluton	95.0	205.6	2.11	20.07	1.3371 ± 0.0155	0.706375 ± 0.000020	0.06334 ± 0.00091	0.512264 ± 0.000016	–7.26	0.705121 ± 0.000025	0.512237 ± 0.000016	–6.13	0.79
202850	Crowded feldspar Boulder Baldy pluton	104.1	1316	0.87	5.49	0.2288 ± 0.0170	0.705102 ± 0.000029	0.09613 ± 0.00031	0.512231 ± 0.000013	–7.90	0.704887 ± 0.000033	0.512189 ± 0.000013	–7.05	1.05
202869	Crowded feldspar Boulder Baldy pluton	127.3	1134	2.87	17.62	0.3248 ± 0.0270	0.705579 ± 0.000021	0.09828 ± 0.00107	0.512311 ± 0.000014	–6.34	0.705274 ± 0.000033	0.512269 ± 0.000014	–5.51	0.97
202883	Weakly mineralized granodiorite/quartz monzodiorite of Miller Mountain	73.9	732.2	2.00	12.08	0.2919 ± 0.0034	0.706591 ± 0.000020	0.09996 ± 0.00040	0.511760 ± 0.000023	–17.09	0.706317 ± 0.000020	0.511717 ± 0.000023	–16.28	1.71

Table 3. Rubidium, strontium, samarium, and neodymium concentrations; and strontium and neodymium isotopic compositions of selected samples from the Big Belt Mountains, Montana.—Continued

[ε_{Nd}, epsilon neodymium; Ga, giga-annum; Ma, mega-annum; Nd, neodymium; ppm, parts per million; Rb, rubidium; Sm, samarium; Sr, strontium; T_{DM}, depleted mantle model age]

Sample	Formation[1]	Rb ppm	Sr ppm	Sm ppm	Nd ppm	$^{87}Rb/^{86}Sr$	$^{87}Sr/^{86}Sr$	$^{147}Sm/^{144}Nd$	$^{143}Nd/^{144}Nd$	ε_{Nd}	Initial $^{87}Sr/^{86}Sr$	Initial $^{143}Nd/^{144}Nd$[3]	Initial ε_{Nd}[2,3]	T_{DM} (Ga)[4]
202939	Feldspar porphyry south of Mount Edith	39.0	962.7	3.48	20.74	0.1172 ± 0.0020	0.707388 ± 0.000042	0.10139 ± 0.00041	0.511808 ± 0.000015	–16.15	0.707278 ± 0.000042	0.511764 ± 0.000015	–15.35	1.66
202958	Proterozoic lamprophyre dike	45.7	186.2	6.08	24.38	0.7106 ± 0.0279	0.713600 ± 0.000020	0.15071 ± 0.00089	0.512518 ± 0.000015	–2.30	0.712934 ± 0.000033	0.512453 ± 0.000015	–1.91	1.26
202863A	Weakly mineralized rock from Porcupine prospect; iron	4.6	7.6	1.37	11.91	1.7337 ± 0.0118	0.708885 ± 0.000046	0.06963 ± 0.00008	0.512081 ± 0.000021	–10.83	0.707259 ± 0.000047	0.512051 ± 0.000021	–9.76	1.02
202849	Fluorite-Normandy prospect	0.2	4.3	0.05	0.66	0.1142 ± 0.0011	0.706776 ± 0.000021	0.04176 ± 0.00132	0.512280 ± 0.000100	–6.94	0.706669 ± 0.000021	0.512262 ± 0.000100	–5.64	0.68
202868	Mineralized hornblende quartz monzodiorite east of Porcupine prospect	107.4	765.2	1.96	12	0.4059 ± 0.0311	0.705572 ± 0.000019	0.09867 ± 0.00039	0.512203 ± 0.000015	–8.45	0.705191 ± 0.000035	0.512160 ± 0.000015	–7.62	1.11
202873A	Vein in Mesoproterozoic Newland Formation, massive	33.1	487.8	2.22	9.88	0.1966 ± 0.0017	0.712949 ± 0.000023	0.13590 ± 0.00018	0.511643 ± 0.000015	–19.37	0.712765 ± 0.000023	0.511584 ± 0.000015	–18.86	2.75
202873B	Vein in Mesoproterozoic Newland Formation, iron	70.3	125.7	0.63	5.23	1.6209 ± 0.0181	0.720275 ± 0.000020	0.07309 ± 0.00024	0.512347 ± 0.000014	–5.64	0.718755 ± 0.000026	0.512315 ± 0.000014	–4.60	0.76
202880	Mineralized Mesoproterozoic Newland Formation north of Boulder Baldy	61.1	357.1	0.40	3.25	0.4955 ± 0.0162	0.713768 ± 0.000016	0.07516 ± 0.00045	0.512333 ± 0.000015	–5.91	0.713303 ± 0.000022	0.512301 ± 0.000015	–4.89	0.78
202860	Mineralized Mesoproterozoic Newland Formation at Bigler prospect	110.5	346.7	2.04	10.58	0.9225 ± 0.0627	0.717865 ± 0.000022	0.11626 ± 0.00036	0.511559 ± 0.000015	–21.01	0.717000 ± 0.000063	0.511509 ± 0.000015	–20.33	2.31
202862	Mineralized Mesoproterozoic Newland at Snowbank prospect	52.6	440.1	2.17	11.66	0.3457 ± 0.0130	0.709525 ± 0.000019	0.11233 ± 0.00043	0.511599 ± 0.000015	–20.23	0.709201 ± 0.000023	0.511551 ± 0.000015	–19.52	2.16
202856	Mesoproterozoic Newland Formation	58.7	165.7	3.68	21.34	1.0270 ± 0.0103	0.739809 ± 0.000021	0.10401 ± 0.00021	0.511363 ± 0.000014	–24.83	0.738846 ± 0.000023	0.511318 ± 0.000014	–24.05	2.32

[1]From du Bray and Snee (2002).

[2]Deviation in parts per 10,000 from calculated bulk-earth values at the present day and at 66 Ma (From DePaolo and Wasserburg, 1976).

[3]Initial ratios calculated using an age of 66 Ma.

[4]Depleted-mantle model age (mantle-separation age) (From DePaolo, 1981).

Table 4. Uranium-thorium-lead concentrations and lead isotopic compositions of selected samples from the Big Belt Mountains, Montana.

[Ma, mega-annum; Pb, lead; ppm, parts per million; Th, thorium; U, uranium]

Sample	Formation[1]	U ppm	Th ppm	Pb ppm	$^{238}U/^{204}Pb$	$^{232}Th/^{204}Pb$	$^{206}Pb/^{204}Pb$	$^{207}Pb/^{204}Pb$	$^{208}Pb/^{204}Pb$	$^{207}Pb/^{206}Pb$	$^{208}Pb/^{206}Pb$	Initial[2] $^{206}Pb/^{204}Pb$	Initial[2] $^{207}Pb/^{204}Pb$	Initial[2] $^{208}Pb/^{204}Pb$
202870	Hornblende quartz monzodiorite of Mount Edith	0.89	4.20	15.78	3.5 ± 0.1	17.2 ± 0.5	17.988 ± 0.022	15.475 ± 0.023	37.857 ± 0.076	0.86033 ± 0.00061	2.1046 ± 0.0030	17.952 ± 0.022	15.474 ± 0.023	37.801 ± 0.076
202885	Hornblende quartz monzodiorite of Mount Edith	2.59	9.33	14.72	11.0 ± 0.4	40.8 ± 0.9	17.899 ± 0.022	15.451 ± 0.023	37.785 ± 0.076	0.86320 ± 0.00061	2.1109 ± 0.0030	17.786 ± 0.022	15.445 ± 0.023	37.651 ± 0.076
202886	Hornblende quartz monzodiorite of Mount Edith	0.90	4.14	16.51	3.4 ± 0.1	16.2 ± 0.4	17.912 ± 0.022	15.467 ± 0.023	37.765 ± 0.076	0.86348 ± 0.00061	2.1084 ± 0.0030	17.877 ± 0.022	15.465 ± 0.023	37.712 ± 0.076
202854	Core/inner zone Boulder Baldy pluton: biotite granodiorite	0.76	3.61	13.19	3.5 ± 0.1	17.2 ± 0.4	16.856 ± 0.021	15.339 ± 0.023	37.161 ± 0.075	0.90997 ± 0.00064	2.2046 ± 0.0031	16.820 ± 0.021	15.337 ± 0.023	37.105 ± 0.075
202853	Core/inner zone Boulder Baldy pluton: biotite granodiorite	0.69	1.65	12.16	3.5 ± 0.1	8.5 ± 0.2	16.808 ± 0.021	15.308 ± 0.023	37.060 ± 0.074	0.91077 ± 0.00064	2.2049 ± 0.0031	16.772 ± 0.021	15.306 ± 0.023	37.032 ± 0.074
202934	Intermediate zone Boulder Baldy pluton: hornblende quartz monzodiorite	1.25	4.65	15.33	5.1 ± 0.2	19.5 ± 0.4	17.796 ± 0.022	15.429 ± 0.023	37.739 ± 0.076	0.86700 ± 0.00061	2.1207 ± 0.0030	17.743 ± 0.022	15.426 ± 0.023	37.676 ± 0.076
202951	Intermediate zone Boulder Baldy pluton: hornblende quartz monzodiorite	1.45	4.23	14.76	6.1 ± 0.2	18.5 ± 0.4	18.004 ± 0.022	15.444 ± 0.023	37.803 ± 0.076	0.85783 ± 0.00061	2.0997 ± 0.0030	17.941 ± 0.022	15.441 ± 0.023	37.743 ± 0.076
202864	Outer zone Boulder Baldy pluton: quartz monzonite, magmatic texture	—	—	—	—	—	18.848 ± 0.013	15.544 ± 0.015	38.923 ± 0.049	0.82471 ± 0.00025	2.0652 ± 0.0013	—	—	—
202945	Outer zone Boulder Baldy pluton: monzodiorite, magmatic texture	3.80	28.80	26.57	9.1 ± 0.4	71.1 ± 1.8	18.646 ± 0.023	15.534 ± 0.023	38.264 ± 0.077	0.83308 ± 0.00059	2.0521 ± 0.0029	18.553 ± 0.023	15.529 ± 0.023	38.032 ± 0.077
202882	Outer zone Boulder Baldy pluton: aegirine quartz monzonite, partly recrystallized	2.85	17.27	19.38	9.4 ± 0.4	58.7 ± 1.2	18.788 ± 0.023	15.534 ± 0.024	38.417 ± 0.077	0.82682 ± 0.00058	2.0448 ± 0.0029	18.691 ± 0.024	15.530 ± 0.024	38.225 ± 0.077
202932	Outer zone Boulder Baldy pluton: quartz syenite, recrystallized and metasomatized	—	—	—	—	—	18.745 ± 0.011	15.566 ± 0.014	38.508 ± 0.046	0.83037 ± 0.00025	2.0543 ± 0.0012	—	—	—
202948	Aplite from outer zone of Boulder Baldy pluton	5.06	17.27	43.20	7.5 ± 0.4	26.3 ± 1.4	18.571 ± 0.025	15.569 ± 0.025	38.419 ± 0.087	0.83838 ± 0.00061	2.0688 ± 0.0035	18.494 ± 0.025	15.566 ± 0.025	38.333 ± 0.087
202850	Crowded feldspar Boulder Baldy pluton	2.88	6.63	29.76	6.1 ± 0.2	14.6 ± 0.3	18.508 ± 0.023	15.508 ± 0.023	38.179 ± 0.076	0.83792 ± 0.00059	2.0628 ± 0.0029	18.445 ± 0.023	15.505 ± 0.023	38.132 ± 0.076
202869	Crowded feldspar Boulder Baldy pluton	6.93	11.26	29.22	15.0 ± 0.6	25.3 ± 0.5	18.586 ± 0.023	15.526 ± 0.023	38.273 ± 0.077	0.83538 ± 0.00059	2.0593 ± 0.0029	18.431 ± 0.024	15.519 ± 0.023	38.191 ± 0.077
202883	Weakly mineralized granodiorite/ quartz monzodiorite of Miller Mountain	0.84	4.14	16.89	3.1 ± 0.1	15.8 ± 0.4	17.663 ± 0.022	15.422 ± 0.023	37.899 ± 0.076	0.87313 ± 0.00062	2.1457 ± 0.0031	17.632 ± 0.022	15.421 ± 0.023	37.848 ± 0.076
202939	Feldspar porphyry south of Mount Edith	1.57	7.39	11.92	8.2 ± 0.3	40.0 ± 0.8	17.873 ± 0.022	15.484 ± 0.023	37.846 ± 0.076	0.86635 ± 0.00061	2.1176 ± 0.0030	17.788 ± 0.022	15.480 ± 0.023	37.715 ± 0.076
202958	Proterozoic lamprophyre dike	0.91	4.52	7.53	7.8 ± 0.3	39.8 ± 1.0	18.829 ± 0.026	15.610 ± 0.025	38.712 ± 0.081	0.82907 ± 0.00059	2.0560 ± 0.0029	18.749 ± 0.026	15.607 ± 0.026	38.582 ± 0.081
202863A	Weakly mineralized rock from Porcupine prospect; iron	0.49	1.33	17.61	1.8 ± 0.1	4.9 ± 0.1	17.884 ± 0.022	15.538 ± 0.024	37.561 ± 0.075	0.86883 ± 0.00063	2.1002 ± 0.0030	17.866 ± 0.022	15.538 ± 0.024	37.545 ± 0.075

Table 4. Uranium-thorium-lead concentrations and lead isotopic compositions of selected samples from the Big Belt Mountains, Montana.—Continued

[Ma, mega-annum; Pb, lead; ppm, parts per million; Th, thorium; U, uranium]

Sample	Formation[1]	U ppm	Th ppm	Pb ppm	$^{238}U/^{204}Pb$	$^{232}Th/^{204}Pb$	$^{206}Pb/^{204}Pb$	$^{207}Pb/^{204}Pb$	$^{208}Pb/^{204}Pb$	$^{207}Pb/^{206}Pb$	$^{208}Pb/^{206}Pb$	Initial[2] $^{206}Pb/^{204}Pb$	Initial[2] $^{207}Pb/^{204}Pb$	Initial[2] $^{208}Pb/^{204}Pb$
202849	Fluorite-Normandy prospect	1.30	1.85	35.00	2.3 ± 0.1	3.4 ± 0.1	18.274 ± 0.023	15.527 ± 0.023	38.045 ± 0.076	0.84968 ± 0.00060	2.0819 ± 0.0030	18.250 ± 0.023	15.526 ± 0.023	38.033 ± 0.076
202868	Mineralized hornblende quartz monzodiorite east of Porcupine prospect	3.06	21.00	22.38	8.7 ± 0.3	61.3 ± 1.3	18.417 ± 0.023	15.500 ± 0.023	38.219 ± 0.077	0.84163 ± 0.00060	2.0752 ± 0.0029	18.328 ± 0.023	15.496 ± 0.023	38.019 ± 0.077
202873A	Vein in Mesoproterozoic Newland Formation, massive	0.76	1.67	5.22	9.1 ± 0.4	20.8 ± 0.7	18.256 ± 0.023	15.581 ± 0.024	37.747 ± 0.077	0.85343 ± 0.00061	2.0676 ± 0.0030	18.163 ± 0.024	15.576 ± 0.024	37.679 ± 0.077
202873B	Vein in Mesoproterozoic Newland Formation, iron	11.21	30.60	5.00	155.6 ± 5.5	438.9 ± 21.0	22.404 ± 0.028	15.804 ± 0.024	41.087 ± 0.083	0.70540 ± 0.00050	1.8339 ± 0.0026	20.803 ± 0.063	15.728 ± 0.024	39.651 ± 0.107
202880	Mineralized Mesoproterozoic Newland north of Boulder Baldy	5.09	17.16	56.56	5.6 ± 0.2	19.4 ± 0.6	17.717 ± 0.022	15.545 ± 0.023	37.222 ± 0.075	0.87740 ± 0.00062	2.1009 ± 0.0030	17.660 ± 0.022	15.542 ± 0.023	37.158 ± 0.075
202860	Mineralized Mesoproterozoic Newland at Bigler prospect	0.97	4.79	5.32	11.5 ± 0.5	58.6 ± 1.2	18.410 ± 0.024	15.590 ± 0.024	37.921 ± 0.077	0.84678 ± 0.00060	2.0597 ± 0.0029	18.292 ± 0.024	15.584 ± 0.024	37.729 ± 0.078
202862	Mineralized Mesoproterozoic Newland at Snowbank prospect	6.64	3.86	85.70	4.9 ± 0.2	2.9 ± 0.1	18.311 ± 0.022	15.516 ± 0.023	38.050 ± 0.076	0.84735 ± 0.00060	2.0780 ± 0.0029	18.261 ± 0.023	15.513 ± 0.023	38.041 ± 0.076
202856	Mesoproterozoic Newland Formation	2.31	8.71	2.46	61.7 ± 2.4	240.1 ± 6.5	20.501 ± 0.029	15.808 ± 0.026	38.712 ± 0.085	0.77109 ± 0.00055	1.8883 ± 0.0029	19.867 ± 0.038	15.778 ± 0.026	37.927 ± 0.088

[1]From du Bray and Snee (2002).

[2]Initial ratios calculated using an age of 66 Ma.

radiogenic Nd, than other rocks from the Big Belt Mountains. Consequently, hydrothermal fluids that equilibrated with the Newland Formation rocks in the southern part of the Big Belt Mountains produced mineralized rocks with significantly enhanced radiogenic Sr and subtly more radiogenic Nd. These mixing relations, involving a component equilibrated with Newland Formation rocks, are also well supported by Pb isotope compositions of these rocks (fig. 3).

In contrast, four mineralized samples from outcrops spatially associated with the intrusive suite of Boulder Baldy define an isotopically distinct mixing array. The ε_{Nd} values for these samples are similar to those characteristic of the outer and intermediate zones of the intrusive suite of Boulder Baldy rocks; however, their Sr_i values are significantly more radiogenic. The sample with the most radiogenic Sr (Sr_i=0.718755) contains abundant secondary iron oxide coatings on fractures, whereas the single sample with a distinctly elevated ε_{Nd} value (–9.76) is weakly altered granitoid rock similar to the quartz monzodiorite of Mount Edith; the sample's isotopic similarity, particularly the similarity of its Sr_i values, to the quartz monzodiorite of Mount Edith corroborates its correlation with that pluton. The Nd, Sr, and Pb isotopic data for the four mineralized samples spatially associated with the intrusive suite of Boulder Baldy all consistently indicate that the hydrothermal alteration of the outer zone rocks contributed to the isotopic character of the spatially associated mineralized rocks. However, these isotopic values all indicate a source component that was not previously identified in the Big Belt Mountains.

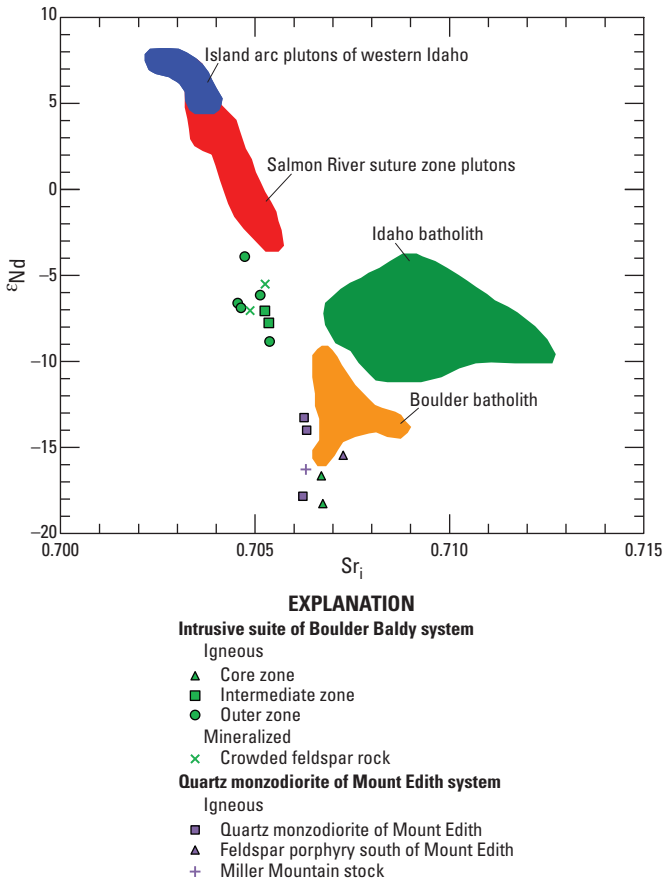

Figure 4. Variation diagram showing ε_{Nd} and Sr_i values for intrusive rocks in the central Big Belt Mountains, Montana, relative to those for Mesozoic island arc plutons of western Idaho and Cretaceous plutons in the Salmon River suture zone and Boulder and Idaho batholiths (From Unruh and others, 2008). (ε_{Nd}, neodymium isotope composition; Sr_i, initial strontium isotope ratio)

Regional Isotopic Systematics

Radiogenic isotope data for intrusive rocks in the Big Belt Mountains underscore their relative uniqueness compared to other similarly aged Cretaceous intrusive rocks in Idaho and Montana. The Sr_i values for the Big Belt rocks are more radiogenic than are the values for the island arc plutons of western Idaho and plutonic rocks of the Salmon River suture zone but are less radiogenic than Boulder and Idaho batholith rocks (fig. 4). The ε_{Nd} values for Late Cretaceous intrusions in the Big Belt Mountains overlap those of the Boulder and Idaho batholiths but are more radiogenic than are those for the island arc plutons of western Idaho and plutonic rocks of the Salmon River suture. Their similar ages and proximity suggest that intrusive rocks of the Boulder batholith and the Big Belt Mountains had similar sources and petrogenetic histories. However, Sr_i values are consistent with intrusive rocks in the Big Belt Mountains that have a less evolved source, including some contribution from the asthenospheric mantle and (or) being less contaminated by crustal assimilants than rocks of the Boulder batholith. Relative $^{206}Pb/^{204}Pb$ variations are principally a function of the age of the associated igneous rocks and their sources, whereas $^{207}Pb/^{204}Pb$ and $^{208}Pb/^{204}Pb$ variations principally reflect radiogenic Pb compositions (the extent of geochemical evolution) of the magmatic source as well as the Pb isotopic composition of crustally derived contaminants. Initial $^{207}Pb/^{204}Pb$, and to a lesser extent $^{208}Pb/^{204}Pb$, values for Late Cretaceous intrusive rocks in the central Big Belt Mountains are systematically less radiogenic than are the values for most other Late Cretaceous rocks in Idaho and Montana (fig. 5). Consequently, among igneous rocks in Idaho and Montana, those in the central Big Belt Mountains, especially the outer and intermediate zones of the intrusive suite of Boulder Baldy, are the least contaminated by assimilation of isotopically evolved crustal components and include a greater proportion of subcontinental, lithospheric mantle-derived material. In addition, the contrast with plutonic rocks of the Boulder batholith is once again noteworthy.

Synthesis

Epsilon neodymium (ε_{Nd}) and initial strontium isotope ratio (Sr_i) data for Late Cretaceous igneous rocks in the Big Belt Mountains define two distinct groups. The outer and intermediate zone components of the intrusive suite of Boulder

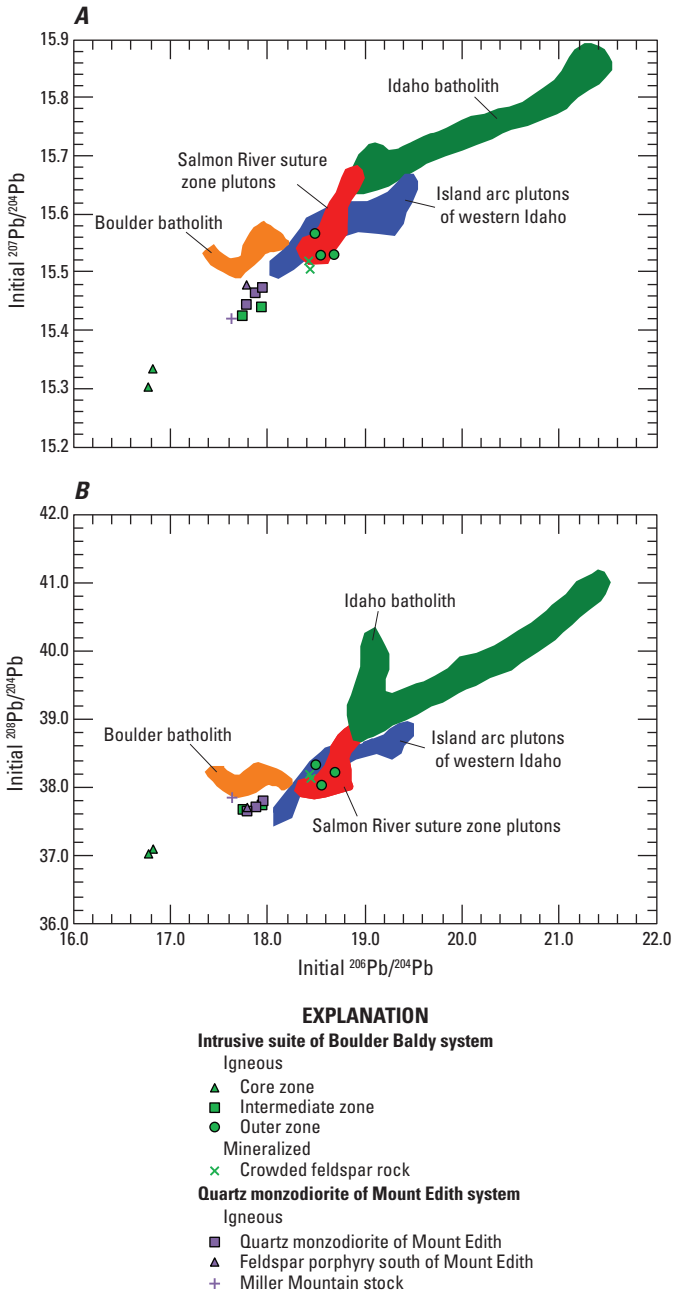

Figure 5. Variation diagram showing initial lead isotope compositions of intrusive rocks in the central Big Belt Mountains, Montana, relative to those for Mesozoic island arc plutons of western Idaho and Cretaceous plutons in the Salmon River suture zone and Boulder and Idaho batholiths (From Unruh and others, 2008). (Pb, lead)

Baldy define a less radiogenic population, whereas the quartz monzodiorite of Mount Edith and the core zone of the intrusive suite of Boulder Baldy define a more radiogenic population. In contrast, initial lead isotope compositions of these rocks are somewhat more complicated. Specifically, the outer, intermediate, and core zones of the intrusive suite of Boulder Baldy define three progressively less radiogenic populations with initial lead isotope values for the intermediate zone overlapping those of the quartz monzodiorite of Mount Edith. As a whole, these radiogenic isotope data suggest distinctly different sources and crustal contaminants for magmas represented by the quartz monzodiorite of Mount Edith and particular zones within the intrusive suite of Boulder Baldy; these relations imply highly localized, source region isotopic heterogeneity and variable contamination by isotopically diverse crustal assimilants. Distinctive ε_{Nd}, Sr_i, $^{208}Pb/^{204}Pb$, and $^{206}Pb/^{204}Pb$ values for the quartz monzodiorite of Mount Edith, the intermediate zone of the intrusive suite of Boulder Baldy, and especially the core zone of the intrusive suite of Boulder Baldy are consistent with the petrogenesis of the associated magmas involving an old, Archean to earliest Proterozoic, rubidium- and uranium-depleted component composed of mafic to intermediate basement. In addition, the strontium, neodymium, and lead isotopic systematics in magmas represented by these intrusive rocks were not coupled. On a regional basis, Late Cretaceous igneous rocks in the Big Belt Mountains have ε_{Nd} values that are similar to those of the Boulder and Idaho batholiths but are more radiogenic than is characteristic of Late Cretaceous intrusive rocks in central to western Idaho. At any given $^{206}Pb/^{204}Pb$ value, $^{208}Pb/^{204}Pb$, and especially $^{207}Pb/^{204}Pb$, values are less radiogenic than are those for most Late Cretaceous intrusive rocks in Idaho and Montana, which suggests that petrogenesis of the associated magmas involved greater subcontinental lithospheric mantle-derived contributions and lesser crustal contamination.

Radiogenic isotope data for all altered and mineralized rocks in the Big Belt Mountains define two distinct mineralization events. Altered and mineralized rocks associated with the quartz monzodiorite of Mount Edith appear to represent a mixing array that reflects hydrothermal fluids dominated by inputs from the quartz monzodiorite but also involves a component that equilibrated with Newland Formation rocks. This mixing array depicts fluids relatively radiogenic with respect to ε_{Nd}, Sr_i, $^{207}Pb/^{204}Pb$, and to a lesser extent, $^{208}Pb/^{204}Pb$. The other mixing array pertains to altered and mineralized rocks associated with the intrusive suite of Boulder Baldy. One end of this array is anchored by the isotopic compositions of samples from the outer zone of the intrusive suite of Boulder Baldy and extends, at ε_{Nd} values that are much less radiogenic than those characteristic of the other alteration/mineralization mixing array, to more radiogenic Sr_i values. The reservoir for these relatively low ε_{Nd} but high Sr_i fluids was not identified in the Big Belt Mountains. Only the mixing array associated with components derived from Newland Formation rocks is identifiable among initial lead isotopic values for altered and mineralized rocks in the Big Belt Mountains.

Acknowledgments

Data acquired for this study were produced as part of a mineral resource assessment of the Helena National Forest in Montana that was funded by the U.S. Geological Survey Mineral Resources Program. Oxygen isotope compositions were determined by W.D. Christiansen (U.S. Geological Survey). We gratefully acknowledge W.R. Premo (U.S. Geological Survey) for critical insights he provided concerning interpretations of the radiogenic isotope data presented in this report. Constructive reviews by C.S. Holm-Denoma and R.D. Taylor (both U.S. Geological Survey) are much appreciated and helped clarify data presentation.

References Cited

Bindeman, I., 2008, Oxygen isotopes in mantle and crustal magmas as revealed by single crystal analysis: Reviews in Mineralogy and Geochemistry, v. 69, p. 445–478.

Cantanzaro, E.J., Murphy, T.J., Shields, W.R., and Garner, E.L., 1968, Absolute isotopic abundance ratios of common, equal atom, and radiogenic lead isotopic standards: Journal of Research of the National Bureau of Standards, v. 72A, p. 261–267.

Clayton, R.N. and Mayeda, T.K., 1963, The use of bromine pentafluoride in the extraction of oxygen from oxides and silicates for isotopic analysis: Geochimica et Cosmochimica Acta, v. 27, p. 43–52.

DePaolo, D.J., 1981, A neodymium and strontium isotopic study of the Mesozoic calc-alkaline granitic batholiths of the Sierra Nevada and Peninsular Ranges, California: Journal of Geophysical Research, v. 86, p. 10470–10488.

DePaolo, D.J., and Wasserburg, G.J., 1976, Nd isotopic variations and petrogenetic models: Geophysical Research Letters, v. 3, p. 249–252.

du Bray, E.A., 1995, Geologic map showing distribution of Cretaceous intrusive rocks in the central Big Belt Mountains, Broadwater and Meagher Counties, Montana: U.S. Geological Survey Miscellaneous Field Studies Map MF–2291, scale 1:50,000. [Also available at https://pubs.er.usgs.gov/publication/mf2291.]

du Bray, E.A., and Snee, L.W., 2002, Composition, age, and petrogenesis of Late Cretaceous intrusive rocks in the central Big Belt Mountains, Broadwater and Meagher counties, Montana: U.S. Geological Survey Professional Paper 1657, 30 p. [Also available at https://pubs.er.usgs.gov/publication/pp1657.]

Lang, J.R., Baker, T., Hart, C.J.R., and Mortensen, J.K., 2000, Intrusion-related gold systems: Society of Economic Geology Newsletter, v. 40, p. 1–15.

Ludwig, K.R., 1994, Isoplot—A plotting and regression program for radiogenic-isotope data: U.S. Geological Survey Open-File Report 91–445, version 2.75, October 1994, 45 p. [Also available at https://pubs.er.usgs.gov/publication/ofr91445.]

Lund, K., Aleinikoff, J.N., Kunk, M.J., Unruh, D.M., Zeihen, G.D., Hodges, W.C., du Bray, E.A., and O'Neill, J.M., 2002, SHRIMP U-Pb and $^{40}Ar/^{39}Ar$ age constraints for relating plutonism and mineralization in the Boulder batholith region, Montana: Economic Geology, v. 97, p. 241–267.

Taylor, H. P., Jr., 1968, The oxygen isotope geochemistry of igneous rocks: Contributions to Mineralogy and Petrology, v. 19, p. 1–71.

Todt, W., Cliff, R.A., Hanser, A., and Hofmann, A.W., 1993, Recalibration of NBS lead standards using a $^{202}Pb^{205}Pb$ double spike, *in* Seventh Meeting of the European Union of Geosciences Abstracts, Strasbourg, France, 1993: Oxford, Blackwell Scientific Publishers, p. 396.

Unruh, D.M., Lund, Karen, Kuntz, M.A., and Snee, L.W., 2008, Uranium-lead zircon ages and Sr, Nd, and Pb isotope geochemistry of selected plutonic rocks from western Idaho: U.S. Geological Survey Open-File Report 2008–1142, 37 p. [Also available at https://pubs.er.usgs.gov/publication/ofr20081142.]

Publishing support provided by:
Denver Publishing Service Center
For more information concerning this publication, contact:
Center Director, USGS Central Mineral and Environmental Resources Science Center
Box 25046, Mail Stop 973
Denver, CO 80225
(303) 236-1562
Or visit the Central Mineral and Environmental Resources Science Center Web site at:
http://minerals.cr.usgs.gov/

ISSN 2327-638X (online)
https://doi.org/10.3133/ds1040